Available online at www.sciencedirect.com

ScienceDirect

Ceramics International 40 (2014) 2953–2958

CERAMICS INTERNATIONAL

www.elsevier.com/locate/ceramint

Role of carbon nanotubes on load dependent micro hardness of SWCNT–lead silicate glass composite

S. Ghosh[a], A. Ghosh[a], T. Kar[b], S. Das[a], P.K. Das[c], J. Mukherjee[c], R. Banerjee[c,*]

[a]Department of Physics, Jadavpur University, Jadavpur, Kolkata 700032, India
[b]Department of Materials Science, Indian Association for the Cultivation of Science Jadavpur, Kolkata 700032, India
[c]Central Glass and Ceramic Research Institute, Jadavpur, Kolkata 700032, India

Received 31 July 2013; accepted 3 October 2013
Available online 11 October 2013

Abstract

Single wall carbon nanotubes (SWCNTs) were successfully entrapped in lead silicate glass by the melt quench technique. Variation of micro hardness with load for lead silicate glass and the composites (having different wt% of SWCNTs) show Reverse Indentation Size Effect (RISE). Meyer's law, the proportional specimen resistance (PSR) model and the modified PSR model have been analyzed for the load dependent hardness of the glass and the composites. Incremented elastic recovery in the composites than that of the glass was explained by the appealing cushioning performance of entangled SWCNT bundles. In contrast, higher plastic deformation beneath the indenter in the composites was established by evaluating the recovery resistance of the materials.

Keywords: Reverse Indentation Size Effect; Cushioning effect; Local plastic deformation; Recovery resistance

1. Introduction

Carbon nanotubes have attracted significant attention among the researchers in the fabrication of efficient and smart composite materials [1–3] because of their remarkable physical and mechanical properties. Fabulous stiffness, flexibility and high young modulus of individual Single wall carbon nanotubes (SWCNTs) make them ideal reinforcing agents in polymers [4,5], ceramics [6,7] and glasses [8,9]. From mechanical point of view, hardness is an important property for using a material in structural applications. However, the apparent micro hardness of solids either decreased or increased with increasing indentation test load which are commonly known as normal ISE and reverse ISE (RISE) respectively. Though various reports on load dependent hardness of crystals [10,11], metals [12,13], ceramics [13,14] and glasses [15,16] are available, but a few reports exist on load dependent hardness of CNT incorporated composites [17]. Different mechanical parameters of SWCNT–glass composites were thoroughly analyzed in our previous reports [18,19] which deal with a single concentration of SWCNTs in the glass host. Those earlier observations give the motivation for evaluating the indentation load/size effect in SWCNT–lead silicate glass composites (contain different wt% of SWCNTs) along with the base glass. The fundamental concern of this work was to determine the load dependent and the load independent micro hardness of the specimens. Moreover, the effect of SWCNT concentration in the composites was also examined in this report. Classical Meyer's law, the PSR model and the modified PSR model have been analyzed in this framework to elucidate the most explainable model for this phenomenon. The main interest of this study was to ascertain the function of SWCNTs in this composite, since the basic study of indentation load/size effect for CNT composites is still in the nascent stage.

2. Materials and methods

Commercially available SWCNT of purity: 90%, OD: 1–2 nm, length: 5–20 μm and special surface area: $>400\ m^2/g$ was purchased from Arry, Germany to fabricate SWCNT–lead silicate glass composite. A mixture of aniline, toluene and SWCNTs (0.05–0.1 g) was prepared in a conical flux and heated at reflux until the solution become dark brown [20].

*Corresponding author. Tel.: +91 3324838079x3255; fax.: +91 3324730957.
E-mail address: rajatbanerjee@hotmail.com (R. Banerjee).

0272-8842/$ - see front matter © 2013 Elsevier Ltd and Techna Group S.r.l. All rights reserved.
http://dx.doi.org/10.1016/j.ceramint.2013.10.015

Three different SWCNT solutions were prepared of varying weights of SWCNTs. Lead silicate glass was selected as a host material of following composition SiO_2: 52.7%, PbO: 35.1%, K_2O: 10.1%, Na_2O: 0.5%, BaO: 0.9%, As_2O_3: 0.3%, and Sb_2O_3: 0.4%. The glass transition temperature (T_g) and the softening point of the glass was found to be 560 and 650 °C respectively. Some small pieces of lead silicate glass of weight ~4.2 g were taken in a crucible and properly mixed up with a certain volume of the prepared SWCNT solution. Atmospheric controlled furnace was used to melt the mixture in the crucible at 720–740 °C for 1 h in argon atmosphere and then quickly cooled to room temperature to avoid crystallization. Depending upon the different weights of SWCNTs in the solution, three different SWCNT lead silicate glass composites have been fabricated namely LSCNT-1, LSCNT-2, and LSCNT-3 containing 0.5, 1.2 and 1.5 wt% of SWCNT respectively. The base glass and the aforesaid composites of same dimension was then optically polished and Vicker's indentation [Model No. Leco LH 700] carried out using loads 0.1, 0.15, 0.2, 0.25, 0.5 and 1 N with 10 s dwell time at each test load. 10–12 indents were made on each sample to verify consistency of data.

3. Result and discussion

3.1. Hardness

Fig. 1 shows the hardness values along with the standard deviations for all specimens. It can be seen that all the glass composites had superior hardness than the base glass irrespective of indentation load. Further, the same increasing nature of the hardness values was observed for the increased wt% of SWCNTs in the composites. Another significant fact can be observed from Fig. 1 where the hardness of all the specimens was increased with the increasing load up to a certain limit and then became stable to achieve a constant value. The increase in the hardness in lower load region can be attributed to the Reverse Indentation Size Effect (RISE). Fig. 2 shows the Field Emission Scanning Electron Microscopy (FESEM) images of indentation impressions for the glass and the composites. Furthermore, Fig. 3 (FESEM image) represents the entanglement of the SWCNT bundles and their interaction around the indentation impression. Based on the reports of Liu et. al. [21] and other researchers [22,23] it can be stated that the enormous resilience property and the cushion like behavior of entangled SWCNT bundles are the responsible factors for the incremented hardness of the CNT composites. Comprehensive analysis of this phenomenon and the effects were reported in our previous works [18,19], but the detailed survey of the RISE was not present in those reports. The present paper particularly deals with the above trend correlating the Meyer's law, the PSR model and the modified PSR model.

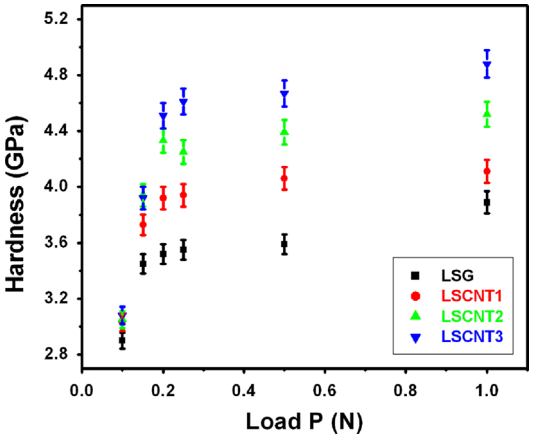

Fig. 1. Hardness versus load graph of Lead silicate glass and three lead silicate glass composites.

3.2. Meyer's law

By this law indentation load 'P' is related to Vickers impression diagonal 'd' as follows:

$$P = Ad^n \tag{1}$$

Where A is a constant and n is Meyer's exponent. According to the law for the load independent hardness of a material n value should be 2. On the other hand, load dependent hardness should result in n value either less than 2 (for ISE) or greater than 2 (for RISE). More deviation of the n value from 2 represents more ISE or RISE in the test material. A and n can be determined from the slope of the curve in Fig. 4. Table 1 shows the linear fit of the ln(P) verses ln(d) data where one can see that the value of n is greater than 2, which invariably proves that our specimen follows RISE. Interestingly our CNT composites show higher RISE than that of the base glass and the composites carry higher trend of n value with increased wt% of SWCNTs.

3.3. PSR model

The constant hardness value at the higher load (Fig. 1) of the specimens could not be explained by the classical Meyer's law and hence we use the PSR model proposed by Li and Bradt [24]. According to this law, there is a polynomial relation between P and d given by

$$P = a_1 d + a_2 d^2 \tag{2}$$

The term a_1 is the contribution of the apparent hardness and related to the elastic deformation properties of a material. On the other hand a_2 originates from the plastic deformation properties of a material and is related to the load independent true hardness (H_T) of a specimen as follows:

$$H_T = ka_2 \tag{3}$$

Where $k = 1.8544$ for Vickers indent. Fig. 5 shows (P/d) versus d plot and their linear fits. Table 2 shows the linear regression analysis along with their calculated H_T values where one can see the inconsistency in the a_1 value (for the LSCNT-1). Further, it was observed that the H_T values were higher than the experimental hardness values for all the specimens.

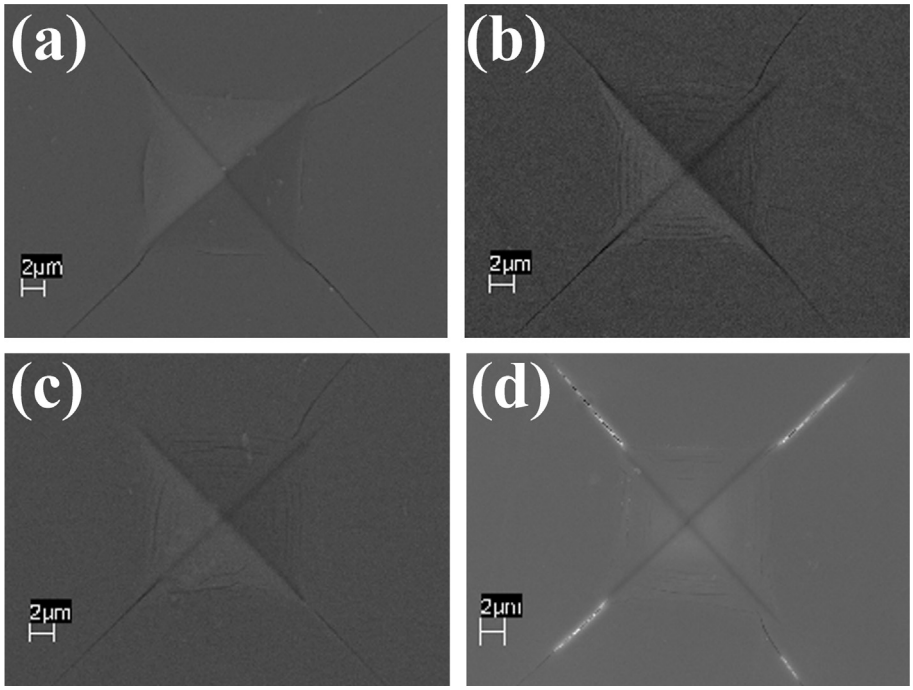

Fig. 2. FESEM images of indentation impressions (a) LSG[19], (b) LSCNT 1, (c) LSCNT 2, and (d)LSCNT 3[19].

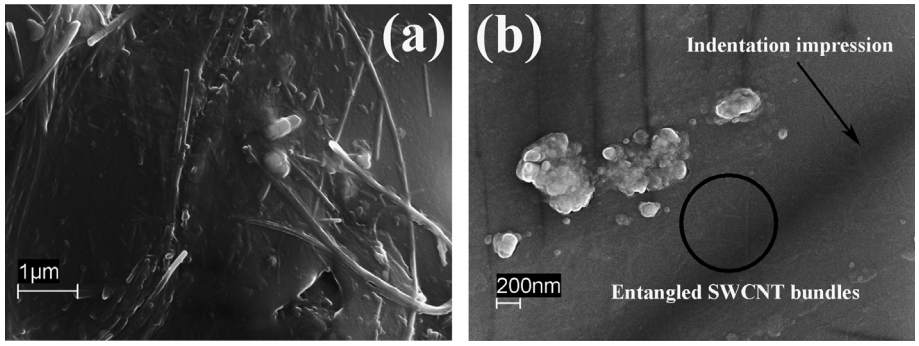

Fig. 3. FESEM images of SWCNT–lead silicate glass composite shows the random distribution and the entanglement of SWCNT bundles (a) in non indented sample and (b) in indented sample.

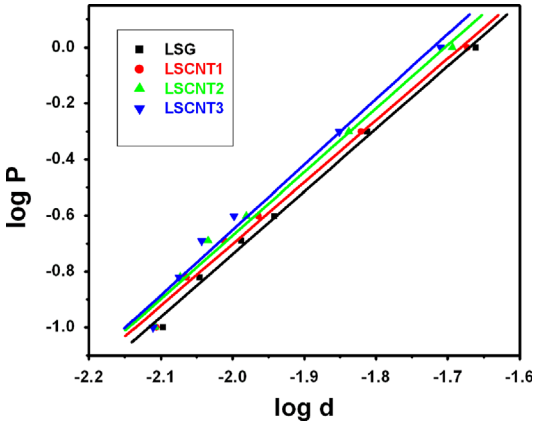

Fig. 4. Plot of log (*P*) versus log (*d*) according to Meyer's law.

The difference between the two set of values may have been originated from the thermal and/or machining induced residual stresses in the materials.

Table 1
Regression analysis of experimental data for all specimens using Meyer's law.

Sample	logA	*n*	R^2
LSG	3.74	2.2	0.997
LSCNT-1	3.71	2.21	0.995
LSCNT-2	3.87	2.27	0.991
LSCNT-3	4.01	2.33	0.989

3.4. Modified PSR model

For precise investigation of the indentation load/size effect on the hardness, researchers frequently used the modified PSR model proposed by Gong et. al. [25] where, they incorporated an additional term related to the residual stress effect due to machining. In many works [17,26] this model turns out to be very much predictive for the comprehensive analysis of the indentation data. Furthermore, previous reports show that the

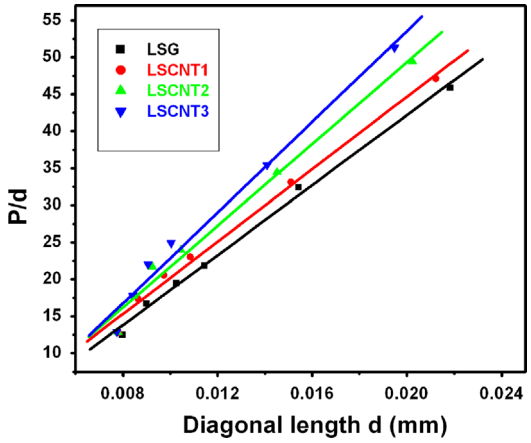

Fig. 5. Plot of (P/d) versus d according to the PSR model.

Table 2
Regression analysis of experimental data for all specimens using the PSR model.

Sample	a_1 (N/mm)	a_2 (N/mm^2)	R^2	H_T (GPa)
LSG	−5.08	2363.19	0.997	4.38
LSCNT-1	−4.23	2443.9	0.995	4.53
LSCNT-2	−5.84	2757.91	0.992	5.11
LSCNT-3	−7.7	3061.09	0.991	5.67

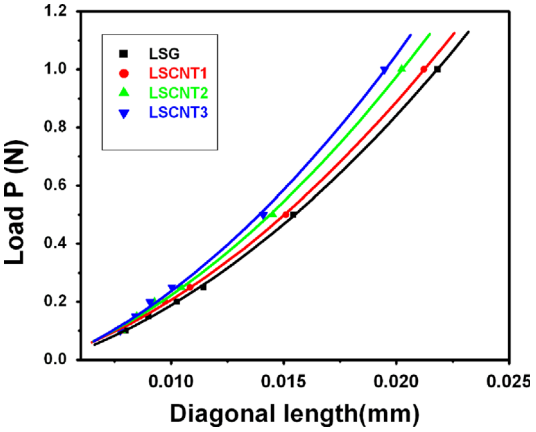

Fig. 6. Plot of P versus d according to the M-PSR model.

RISE was mostly explained by this model [27,28]. According to this model P and d are related as

$$P = P_0 + a_1 d + a_2 d^2 \quad (4)$$

Where P_0 indicates the residual stress appeared in the specimen due to surface machining and a_1, a_2 represents the same physical significance as stated earlier in Eq. (2). Here P_0, a_1 and a_2 can be evaluated from the second order polynomial fit of P and d data plot which is shown in Fig. 6 and results are given in Table 3. It is evident from P_0 values in Table 3 that surface machining and polishing have considerable effect on RISE. The negative values of P_0 for all the specimens indicate

Table 3
Regression analysis of experimental data for all specimens using the M-PSR model.

Sample	P_0 (N)	a_1 (N/mm)	a_2 (N/mm^2)	R^2(GPa)	H_T (GPa)
LSG	−0.08726	8.664	1888.35	0.999	3.51
LSCNT-1	−0.08214	9.207	1964.15	0.999	3.63
LSCNT-2	−0.09662	10.41	2156.61	0.998	4.01
LSCNT-3	−0.11586	12.19	2305.81	0.998	4.28

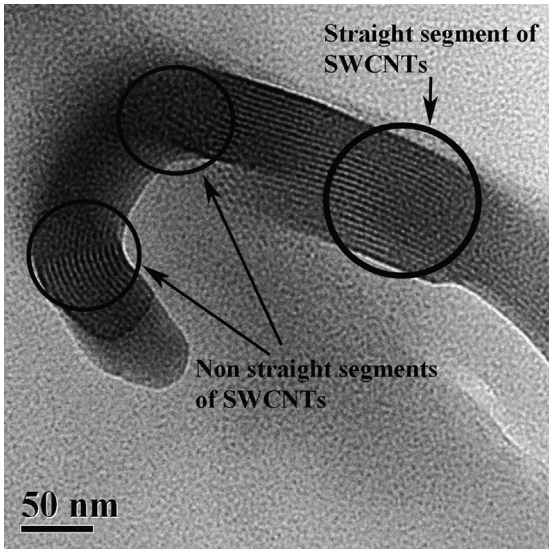

Fig. 7. HRTEM image of SWCNTs inside a bundle.

that stresses were compressive during surface machining and polishing [29]. The values of a_1 and a_2 both increase in composites than the base glass and show the same trend as the concentration of SWCNTs increases in the composite. Glass being a brittle material, hence a plastic deformation under an indentation impression decreases considerably the elastic recovery during unloading. Interestingly one can observe the increasing trend in the values of a_1 and a_2 (Table 3) which indicates the increment of both the parameters plastic deformation and elastic recovery. The cushioning and the toughening behavior of entangled SWCNT bundles are the prime reasons of the enhanced elastic recovery, which further corroborates as one can see the incremented a_1 value in the composites. The effect was more pronounced in the composites containing higher concentration of SWCNTs. The enhanced plastic deformation (represented by a_2 value) in the composites can be explained considering the High Resolution Transmission Electron Microscopy (HRTEM) image (Fig. 7). In this image one can observe straight and nonstraight segments of SWCNTs inside a bundle. Due to rapid cooling of the composite during fabrication, the nanotubes inside the glass host gets forcefully entrapped and become curvy within a bundle. Yakobson et al. [30] reported that any shape change in carbon nanotubes releases high amount of energy. In another report Pathak et al. [31] show that high amount of energy dissipation occurs in

carbon nanotube bundles under compression. In our case SWCNTs (which were just beneath the indenter) changed their shape under compressive stress and releases extra energy. In our proposed theory this additional energy gets added up with the energy of plastic deformation immediately below the indenter, which effectively enhanced the value of a_2 and also the Meyer's exponent 'n' in the composites.

3.5. Recovery resistance

The enhanced local plasticity in the composites is further corroborated by evaluating the recovery resistance (R_S) of the glass and the composites. Bao et al. [32] in their report show that the recovery resistance (R_S) and reduced Young's modulus (E_r) of a material is related as

$$R_s = 2.263(E_r^2/H) \quad (5)$$

where H is the Vickers hardness of a material. Marshall et al. [33] gives the Young's modulus (E) of the specimens from which the E_r values were calculated. According to Bao et al. the recovery resistance of a material increases with increase of plasticity. At 1 N load R_S values of glass and the composites (containing 0.5, 1.2 and 1.5 wt% of SWCNT respectively) were found to be 1.44×10^{12}, 1.48×10^{12}, 1.54×10^{12} and 1.59×10^{12} respectively. Therefore, the increment of R_S values in the composites clearly establishes our proposed theory. Such increment of local plasticity and R_S value in glass composites was discussed in our earlier reports [18,19]. However, the plasticity present in our composite is extremely local and confined within very small area under which one can see a forest of entangled and super resilient SWCNT bundles (Fig. 3). Thus, the plastic deformation cannot dominate over the entire elastic recovery of a material during indentation and hence both a_1 and a_2 values were enhanced in the composites than that of the base glass.

4. Conclusion

Lead silicate glass composites have been fabricated incorporating different wt% of SWCNTs into the glass host by the melt quench technique. Load dependent hardness in the lower load region along with the true hardness was measured for base glass and the composites. RISE was observed for all the specimens and it was more pronounced in the composites than that of the glass. Three empirical law/models were discussed and the M-PSR model was found to be the most predictive in this framework. Cushioning behavior of entangled SWCNT bundles was the main reason for the enhanced hardness and the elastic recovery of the composites. Interestingly, energy dissipation from the curved SWCNTs under compression was responsible for the incremented plastic deformation immediately below the indenter. Thus one can conclude that carbon nanotubes played a decisive role for the indentation load/size effect in SWCNT–lead silicate glass composites.

Acknowledgment

The authors are extremely grateful to Prof. Dr. Indranil Manna, former Director of Central Glass & Ceramic Research institute (CGCRI) for his constant encouragement and support for execution of this work. They also acknowledge Mr. Amit Sarkar, Mr. Sudipta Mandal, Mr. Ranadhir Bose and Mr. Amal Datta from CRF of IIT Kharagpur for sample preparation and attractive HRTEM micrographs and Mr. Ashoke Mandal in ESM division of CGCRI for FESEM micrograph.

References

[1] E.T. Thostenson, W.Z. Li, D.Z. Wang, Z.F. Ren, T.W. Chou, Carbon nanotube/carbon fiber hybrid multiscale composites, Journal of Applied Physics 91 (2002) 6034–6037.
[2] L. Gao, E.T. Thostenson, Z. Zhang, T.W. Chou, Sensing of damage mechanisms in fiber-reinforcedcomposites under cyclic loading using carbon nanotubes, Advanced Functional Materials 19 (2009) 123–130.
[3] M.A. Makeev, S. Sundaresh, D. Srivastavac, Shock-wave propagation through pristine a-SiC and carbon-nanotubereinforced a-SiC matrix composites, Journal of Applied Physics 106 (2009) 014311-1–014311-8.
[4] M. Cadek, J.N. Coleman, V. Barron, K. Hedicke, W.J. Blau, Morphological and mechanical properties of carbon-nanotube-reinforced semicrystalline and amorphous polymer composites, Applied Physics Letters 81 (2002) 5123–5125.
[5] L.S. Schadler, S.C. Giannaris, P.M. Ajayan, Load transfer in carbon nanotube epoxy composites, Applied Physics Letters 73 (1998) 3842–3844.
[6] A. Rishabh, M.R. Joshi, K. Balani, Fractal model for estimating fracture toughness of carbon nanotube reinforced aluminum oxide, Journal of Applied Physics 107 (2010) 123532-1–123532-7.
[7] M. Mazaheri, D. Mari, Z.R. Hesabi, R. Schaller, G. Fantozzi, Multiwalled carbon nanotube/nanostructured zirconia composites: outstanding mechanical properties in a wide range of temperature, Composites Science and Technology 71 (2011) 939–945.
[8] Z. Bian, M.X. Pan, Y. Zhang, W.H. Wang, Carbon-nanotube-reinforced $Zr_{52.5}Cu_{17.9}Ni1_{4.6}Al_{10}Ti_5$ bulk metallic glass composites, Applied Physics Letters 81 (2002) 4739–4741.
[9] B.T.T. Chu, G. Tobias, C.G. Salzmann, B. Ballesteros, N. Grobert, R. I. Todd, M.L.H. Green, Fabrication of carbon-nanotube-reinforced glass–ceramic nanocomposites by ultrasonic in situ sol–gel processing, Journal of Materials Chemistry 18 (2008) 5344–5349.
[10] T. Pal, T. Kar, Vickers microhardness studies of L-arginine halide mixed crystals, Materials Science and Engineering A 354 (2003) 331–336.
[11] G. Feng, A.S. Budiman, W.D. Nix, N. Tamura, J.R. Patel, Indentation size effects in single crystal copper as revealed by synchrotron x-ray microdiffraction, Journal of Applied Physics 104 (2008) 043501-1–043 501-12.
[12] K. Sangwal, B. Surowska, P. Blaziak, Analysis of the indentation size effect in the microhardness measurement of some cobalt-based alloys, Materials Chemistry and Physics 77 (2002) 511–520 (2002).
[13] A.K. Dutta, N. Narasaiah, A.B. Chattopadhyaya, K.K. Roy, The load dependence of hardness in alumina-silver composites, Ceramics International 27 (2001) 407–413.
[14] S.J. Bull, T.F. Page, E.H. Yoffe, An explanation of the indentation size effect in ceramics, Philosophical Magazine Letters 59 (1989) 281–288.
[15] T. Miura, Y. Benino, R. Sato, T. Komatsu, Universal hardness and elastic recovery in Vickers nanoindentation of copper phosphate and silicate glasses, Journal of the European Ceramic Society 23 (2003) 409–416.
[16] H. Li, R.C. Bradt, The effect of indentation-induced cracking on the apparent microhardness, Journal of Materials Science 31 (1996) 1065–1070.

[17] S. Sarkar, P.K. Das, Temperature and load dependent mechanical properties of pressureless sintered carbon nanotube/alumina nanocomposites, Materials Science and Engineering A 531 (2012) 61–69.
[18] S. Ghosh, A. Ghosh, S. Das, T. Kar, P.K. Das, R. Banerjee, Enhanced mechanical properties of single walled carbon nanotube-borosilicate glass composite due to cushioning effect and localized plastic flow, AIP Advances 1 (2011) 042133-1–042133-5.
[19] S. Ghosh, A. Ghosh, T. Kar, S. Das, P.K. Das, R. Banerjee, Cushioning effect, enhanced localized plastic flow and thermal transport in SWCNT–lead silicate glass composite, Chemical Physics Letters 547 (2012) 58–62.
[20] Y. Sun, S.R. Wilson, D.I. Schuster, High dissolution and strong light emission of carbon nanotubes in aromatic amine solvents, Journal of the American Chemical Society 123 (2001) 5348–5349.
[21] Y. Liu, W. Qian, Q. Zhang, A. Cao, Z. Li, W. Zhou, Y. Ma, F. Wei, Hierarchical agglomerates of carbon nanotubes as high-pressure cushions, Nano Letters 8 (2008) 1323–1327.
[22] T. Wei, K. Wang, Z. Fan, W. Qian, F. Wei, Super resilience of a compacted mixture of natural graphite and agglomerated carbon nanotubes under cyclic compression, Carbon 48 (2010) 305–312.
[23] C. Cao, A. Reiner, C. Chung, S.H. Chang, I. Kao, R.V. Kukta, C.S. Korach, Buckling initiation and displacement dependence in compression of vertically aligned carbon nanotube arrays, Carbon 49 (2011) 3190–3199.
[24] H. Li, R.C. Bradt, The microhardness indentation load/size effect in rutile and cassiterite single crystals, Journal of Materials Science 28 (1993) 917.
[25] J. Gong, J. Wu, Z. Guan, Examination of the indentation size effect in low-load Vickers hardness testing of ceramics, Journal of the European Ceramic Society 19 (1999) 2625–2631.
[26] Q. Tang, J. Gong, Effect of porosity on the microhardness testing of brittle ceramics: a case study on the system of NiO–ZrO_2, Ceramics International, 39, 2013, 8751–8759, http://dx.doi.org/10.1016/j.ceramint.2013.04.061.
[27] Z. Peng, J. Gong, H. Miao, On the description of indentation size effect in hardness testing for ceramics: analysis of the nanoindentation data, Journal of the European Ceramic Society 24 (2004) 2193–2201.
[28] T. Kavetskyy, J. Borc, K. Sangwal, V. Tsmots, Indentation size effect and Vickers microhardness measurement of metal-modified arsenic chalcogenide glasses, Journal of Optoelectronics and Advanced Materials 12 (2010) 2082–2091.
[29] J. Gong, Z. Zhao, Z. Guan, H. Miao, Load-dependence of Knoop hardness of Al_2O_3–TiC composites, Journal of the European Ceramic Society 20 (2000) 1895–1900.
[30] B.I. Yakobson, C.J. Brabec, J. Bernholc, Nanomechanics of carbon tubes: instabilities beyond linear response, Physical Review Letters 76 (1996) 2511–2514.
[31] S. Pathak, E.J. Lim, P.P.S.S. Abadi, S. Graham, B.A. Cola, J.R. Greer, Higher recovery and better energy dissipation at faster strain rates in carbon nanotube bundles: an in-Situ study, ACS Nano 6 (2012) 2189–2197.
[32] Y.W. Bao, W. Wang, Y.C. Zhou, Investigation of the relationship between elastic modulus and hardness based on depth-sensing indentation measurements, Acta Materialia 52 (2004) 5397.
[33] D.B. Marshall, T. Noma, A.G. Evans, A simple method for determining elastic-modulus-to-hardness ratios using Knoop indentation measurements, Journal of the American Ceramic Society 65 (1982) C175–C176.